A Radiation and Cryogenic Tolerant Encoder

Nathaniel Rogalskyj

McQuaid Jesuit

LLE Advisors: Gregory Brent, Dave Lonobile

Abstract:

A cryogenic and radiation tolerant encoder was designed and constructed to measure linear displacements with a resolution of 0.1 µm. A coil of wire was fashioned such that the insertion or retraction of an iron rod would result in a change in inductance. An analog circuit, incorporating this variable inductance, generates a ringing signal whose period is analyzed with reference to a 200-MHz counter. Resolution proved to be a function of displacement, smaller displacements yielding higher resolution. Exposure to cryogenic temperatures, although requiring calibration, proved to increase the resolution. Miniaturization of the inductor to a scale useful in laser-fusion target positioning systems is only possible at cryogenic temperatures. A Mathcad document was created to accurately calculate the optimal resolution, capacitance, and the number of turns of the inductor given certain physical input parameters such as temperature, cross-sectional area, length, and gauge.

Introduction:

Nuclear fusion is a possible source for large-scale, clean, virtually limitless energy production. One possible approach for fusion is the irradiation of an implosion target with high power lasers to create the necessary high temperatures and densities. On OMEGA, the implosion target must be held at low, cryogenic temperatures near 20 K. At these temperatures, there is a need for highly sensitive and accurate linear displacement measurements in positioning the capsule into the center of the target chamber. The current solution is centered on the use of a potentiometer, which correlates a measured voltage ratio to a given displacement. The resolution of the potentiometer solution is 0.39 µm. The primary goal of this project was to develop a new encoder that improves upon the current solution. Furthermore there are a number of other applications for an encoder at LLE, with varying physical constraints. A secondary goal of this project was to explore the encoder's design tradeoffs in the context of these other physical

2

constraints. Table 1 lists some of the desired characteristics of the new encoder. Most of them were explored in this work.

Table 1. Desired Characteristics of New Encoder	
Engineering Desirable:	Goal:
High sensitivity	The applications for the encoder require highly accurate measurements. In the case of the target positioning system, the goal was to attain a resolution on a level with or better than 0.39 um.
Cryogenic Tolerance	The applications for the encoder require the above high resolution under extremely cold temperatures, near 20 K.
Physical Adaptability	The applications of the encoder require variable throws, and physical constraints
Radiation Tolerance	Due to use of tritium in the implosion target, and in the lab, the materials of the encoder need to be resistant to tritium corrosion.
Temperature Independence	It is highly desirable for the encoder to not need recalibration

Outline of Design

The goal of the encoder is to detect linear displacements. The system (Figure 1) is composed of a number of different subunits: an RLC circuit incorporating the variable inductance of a set of coils with a magnetic core, an operational amplifier, a voltage offset system and a Field Programmable Gate Array (FPGA).
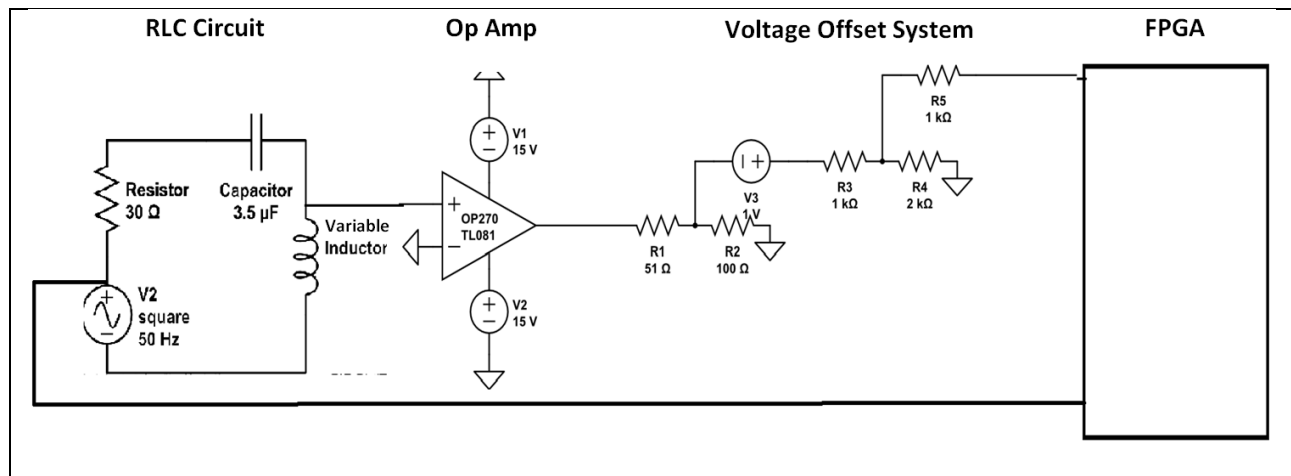

Figure 1. Diagram of the encoder circuitry. The system is composed of an RLC circuit incorporating a variable inductor, an operational amplifier, a voltage offset system, and a FPGA.

The RLC circuit generates a ringing signal. The ringing signal is amplified and squared by the operational amplifier. In the voltage offset system, a DC battery and two voltage dividers scale the signal to the specifications of the FPGA. The FPGA counts the duration that the signal is high with reference to a 200-MHz counter.

Variable Inductor:

A method was required to translate a linear displacement into an electrical property. A linear variable inductor was constructed such that the insertion of a magnetic permeable rod would cause an increase in the inductance. The formula for the inductance, L, of the coil is [1]:

$$L(x) = \frac{u * f(x)N^2 \pi r^2}{l} \quad (Eq. 1)$$

where N is the number of turns, r is the radius of the coil, l is the length of the coil, x is the distance the core has been inserted, and f(x) is a dimensionless function that gives the variation of the inductance with x; f(x)=1 at full insertion. The absolute magnetic permeability is [1]

$$u = u_0 * u_{rel} (Eq. 2)$$

where u_0 is the magnetic permeability of free space and u_{rel} is the relative magnetic permeability. Factors such as magnetic shielding, the external magnetic permeability, the movement of the iron rod insert in warping the magnetic field lines, possible non-linearity between the magnetizing force and the induced magnetic field, and variable frequencies all change the overall measured inductance. The measured value of u_{rel} from the coil setup is:

$$u_{rel} = \frac{Lin}{Lout} \quad (Eq. 3)$$

where Lin is the inductance of the coil with the rod inserted, and $Lout$ is the inductance of the coil with the rod not inserted. The measured values of u_{rel} of the coil setup were much lower than the literature values. Inductor construction materials proved to be minor contributors to this

discrepancy. Five inductor designs, listed in Table 2, together with some of their properties, were investigated.
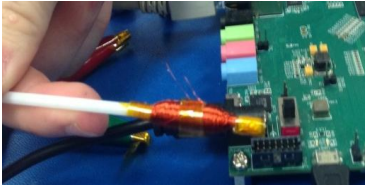
Design Number	Coil Number N	Length (mm)	Radius (mm)	Inductance Not inserted L_{out}	Inductance Fully Inserted L_{in}	Picture
One	1500	300	9.525	2.89uH	6.5uH	
Two	92	239	9.100	3.87uH	11.39uH	
Three	1200	63.21	8.563	5.7896mH	32.901mH	
Four	1800	67.61	8.983	8.009mH	88.981mH	
Five	3600	21.79	2.63	12.706mH	70.787mH	
Table 2. Parameters of the five inductors tested with corresponding pictures.						

The materials for the first two inductor designs were 36 gauge wire, McMaster Carr stainless steel tube, and McMaster Carr High-Speed M2 Iron rod insert. The 36 gauge wire was wrapped around the stainless steel tube. The measurements were done with calipers and the

inductance was taken with an Agilent RLC meter running at 1 kHz frequency. The measured

inductance range from not inserted to fully inserted was too small to gain the resolution that was

the goal. For inductor 2, the u_{rel} was equal to 2.98.

Improving upon the above material choices for inductor 3, the stainless steel mold for the

wires was replaced with a plastic tube. The plastic tube, unlike the stainless steel, did not

interfere with the magnetizing force produced by the coils; the u_{rel} value was 5.68. Similar

construction yielded even higher u_{rel} values. Inductor 4's u_{rel} value was 11.11. Inductor five's

was 5.57.

The higher u_{rel} values allowed for a workable resolution, even though the literature

values for the u_{rel} values of iron are near 5000. Similar results occurred when a Metglas core

whose literature u_{rel} value is near 1,000,000 was tested in inductor 5 and had a measured

u_{rel} value of 30.

Inductor Behavior:

In order to determine the functionality of the device, a number of tests were run on the

inductors. With the third design, a measurement was conducted using calipers and the Agilent

RLC meter running at 1 kHz frequency. The iron rod was stepped through the coil, and each

corresponding inductance measurement was recorded as shown in figure 2. There is a linear

portion of the graph, which can be used for the encoder as the operating range along the coil. In

the final encoder, a mechanical block would limit the throw of the iron rod to this linear range
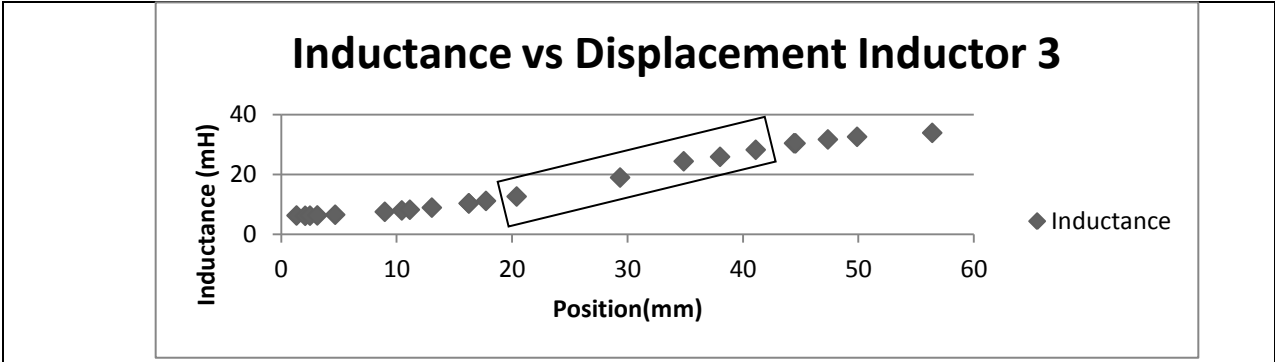
and thereby ensure predictability.

Figure 2. Inductance versus position of the iron rod insert into the inductor. The rectangular box highlights the existence of a portion that is linear. The linearity and the tailing off indicate how the magnetic flux acts as the iron rod is inserted.

The fourth inductor tested had a much more uniform coil density than the third inductor. For inductor 4, the iron rod was stepped through a 20 mm portion of the coil, within the linear range as predicted by figure 2, using a Keyence laser displacement measuring system with an accuracy of one micron. The results are shown below in Figure 3:
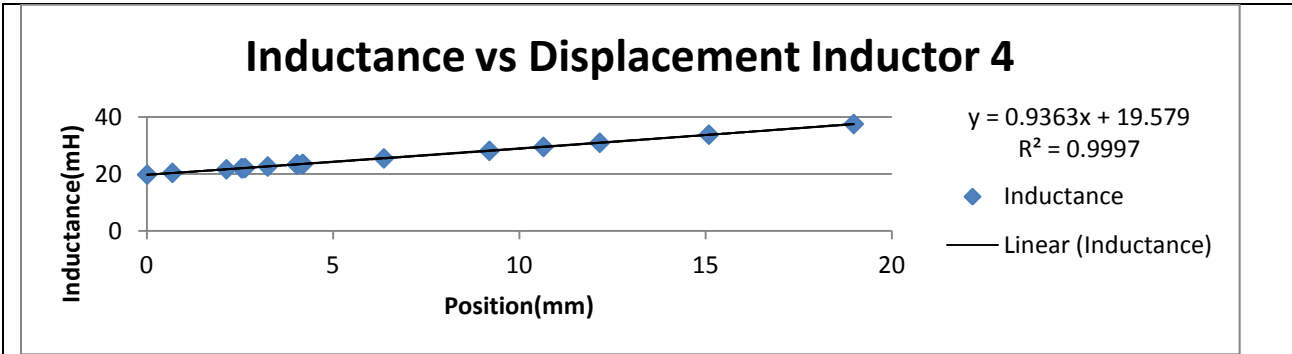

Figure 3. Inductance versus position of the iron rod for inductor 4 over a 20 mm range, centered well in the linear range of the inductor.

RLC Circuit, Operational Amplifier and the FPGA

To determine the position of the rod, a 50 Hz 3V square wave charges a capacitor as shown in yellow in Figure 4. When the power supply square wave drops to the trough, the capacitor discharges and there is an oscillatory voltage signal over the inductor seen in blue, which is fed into the operational amplifier whose output is seen in purple. The op amp output,

adjusted by the voltage offset system, is fed into the FPGA with a 200 MHz clock. The FPGA

then counts the number of clock cycles that the purple wave has a high voltage. The count is then

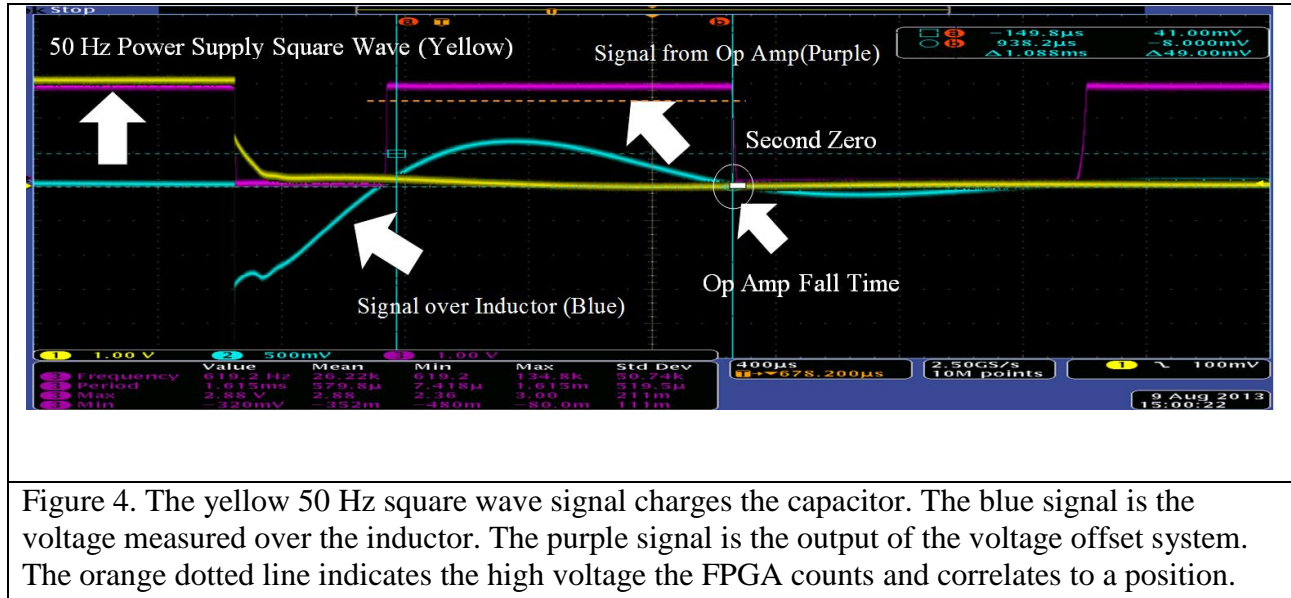correlated to a position of the rod in the inductor.

Figure 4. The yellow 50 Hz square wave signal charges the capacitor. The blue signal is the
voltage measured over the inductor. The purple signal is the output of the voltage offset system.
The orange dotted line indicates the high voltage the FPGA counts and correlates to a position.

The above system works well when the inductance, resistance and capacitance of the

circuit for the full range of the rod insertion cause the blue signal to have well defined

oscillations. If the blue signal does not oscillate, there can be no period reading by the FPGA.

Furthermore, if the slope of the blue signal through its second zero is too shallow, then the op

amp fall time increases asymptotically, as presented in figure 5. A longer fall time for the purple

signal causes a non-linear correlation between the period of the blue signal and the FPGA count.

In addition, the fluctuations of the FPGA count due to noise are greater for higher op amp fall
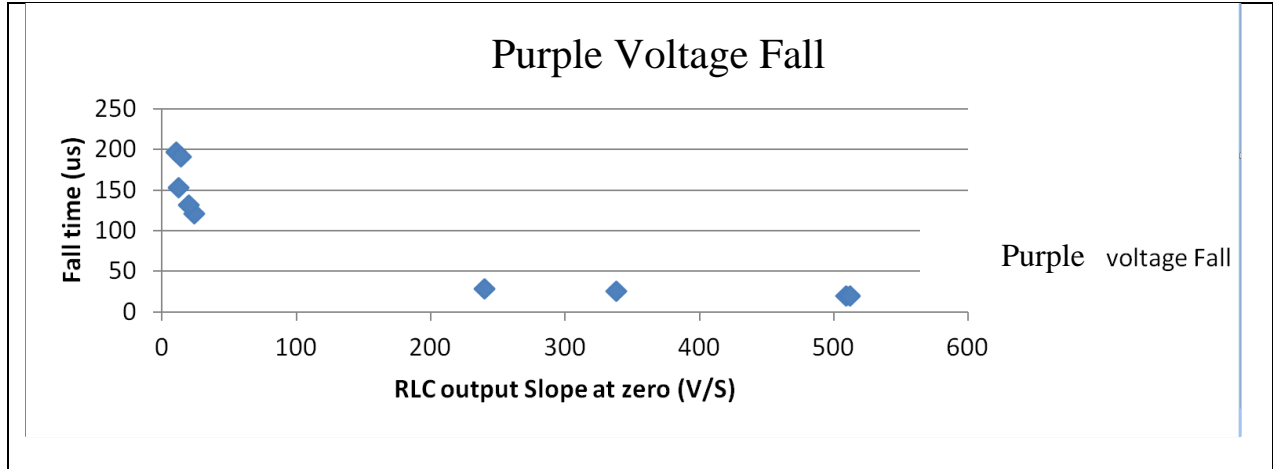
times.

Figure 5. Fall time of the purple voltage signal of figure 4 against the magnitude of the RLC output's slope through the second zero of the period. Lower slope magnitudes cause asymptotically greater fall times, and non-linearity in the FPGA count.

To ensure that the signal over the inductor oscillates and that the fall times are kept under 50 μs, the inductance, resistance and capacitance of the circuit should be bounded such that the magnitude of the slope of the inductor signal at its second zero is greater than 200 V/s. It is therefore important to understand how the inductance, resistance and capacitance correlate to the inductor signal's slope at its second zero, the period of oscillation, and the exponential decay of the voltage.

First, the voltage across the capacitor in an RLC series circuit is [1]:

$$V_c(t) = V_c(\infty) + e^{-\alpha t} * (D_1 cosw_d t + D_2 sinw_d t) \ \ (\text{Eq. 4})$$

$$D_1 = V_c(0) - V_c(\infty)(\text{Eq. 5})$$

$$\alpha = \frac{R}{2L}(\text{Eq. 6})$$

$$w_0 = \frac{1}{\sqrt{L*C}}(\text{Eq. 7})$$

$$D_2 = \frac{V_c{'}(0) + \alpha * D_1}{w_d}(\text{Eq. 8})$$

9

$$w_d = \sqrt{w_0^2 - \alpha^2} \text{(Eq. 9)}$$

where $V_c(\infty)$ is the voltage at t=∞, α is the attenuation coefficient, D_1 is the initial voltage, D_2 is given by the initial current, w_0 is the natural frequency of oscillation, and w_d is the damped frequency. The current through the circuit is [1]:

$$i(t) = C * \frac{dV_c}{dt} \text{(Eq. 10)}$$

The voltage across the inductor in terms of current is [1]:

$$V_L = L * \frac{di}{dt} \text{(Eq. 11)}$$

Performing two differentiations with respect to time:

$$V_L(t) = L * C * e^{-\alpha t} * \{[(\alpha^2 - w_d^2)D_1 - 2\alpha w_d D_2] * \cos(w_d t) + [(\alpha^2 - w_d^2)D_2 + 2\alpha w_d D_1]$$

$$* \sin(w_d * t)\} \text{(Eq. 12)}$$

Given that $\alpha \ll w_0$, i.e. the attenuation must be small for the method to be effective, Eq.9 shows that $w_d \approx w_0$, so the period of oscillation is:

$$T = \frac{2\pi}{w_0} = 2\pi * \sqrt{L * C} \text{(Eq. 13)}$$

The time constant $\tau = 1/\alpha$, or the time it takes for the voltage to decrease by a factor of 1/e is:

$$\tau = \frac{2L}{R} \text{(Eq. 14)}$$

As the magnetic rod slides through the coil, the inductance as shown in figure 3 increases linearly. Therefore, for greater amounts of rod insertion, the ratio of the time constant τ to the period T becomes greater:

$$\frac{\tau}{T} = \frac{\sqrt{L}}{\pi * R * \sqrt{C}} \text{(Eq. 15)}$$

This results in a greater magnitude of the signal's slope at the second zero. The values of inductance, resistance and capacitance are then selected using the lowest values of the inductance corresponding to the magnetic rod being fully retracted. This condition was confirmed with testing as issues with non-linear fall times and lack of oscillations only occurred with no core inserted. The restrictive inductance is then taken from Eq.1, when x=0.

Because resistance only adds to damping, there is no need to add a resistor to the circuit. The only resistance then is the internal resistance of the inductor. The internal resistance of the inductor is:

$$R = 2\pi r * N * \theta \quad (\text{Eq. 16})$$

where θ is the resistance per unit length, dependent upon temperature and gauge of wire.

By taking the derivative of $V_L(t)$ and substituting in the time of the second zero, an inequality can be created that links the minimum 200 V/s slope to the construction characteristics of the inductor and the choice of capacitor. A good approximation to the derivative of $V_L(t)$ can be obtained from Eq. 12 for the usual case where $\alpha \ll w_0$ keeping just the terms in w_d^2:

$$V_L(t) = -w_d^2 * L * C * e^{-\alpha t} * [D_1 \cos(w_d * t) + D_2 \sin(w_d * t)] (\text{Eq. 17})$$

Differentiating,

$$V_L{}'(t) = -w_d^3 * L * C * e^{-\alpha t} * [-D_1 \sin(w_d * t) + D_2 \cos(w_d * t)] (\text{Eq. 18})$$

The time of the second zero, $V_L = 0$ is:

$$t_0 = \frac{\text{atan}\left(\frac{-D_1}{D_2}\right) + \pi}{w_d} (\text{Eq. 19})$$

Therefore the capacitance, inductance and resistance must satisfy the inequality:

$$200 \frac{V}{s} < |V_L{}'(t_0)| = w_d^3 * L * C * e^{-\alpha t_0} * [-D_1 \sin(w_d t_0) + D_2 \cos(w_d t_0)] (\text{Eq. 20})$$

The requirement that the damping be small in comparison with the oscillation frequency can be expressed in terms of the damping coefficient $\delta = \alpha / w_d$:

$$\delta = \frac{R}{2} * \sqrt{\frac{C}{L}} \quad (\text{Eq. } 21)$$

It was found that circuits that had damping coefficients under 0.2 and sufficiently large D_1 and D_2 had the necessary slopes to maintain a well defined oscillation, and avoid non-linearity with op amp fall times.

The values of capacitance, inductance and resistance also determine the resolution of the system. The goal then in the construction of the inductor and the circuit is to maximize the resolution while maintaining the inequality stated in Eq.20 above. The resolution is equivalent to how much of a movement of the iron rod there is per clock cycle. The resolution is:

$$Resolution = \frac{\Delta X}{\Delta T} * \frac{1}{Clockspeed} (\text{Eq. } 22)$$

$$\Delta T = \frac{2\pi}{w_{in}} - \frac{2\pi}{w_{out}} (\text{Eq. } 23)$$

where w_{in} and w_{out} are the oscillation frequencies with the rod in and out, respectively. Furthermore,

$$Resolution = \frac{l}{2\pi\sqrt{\frac{\pi * r^2 * N^2}{l} * C} * (\sqrt{u_0 * u_{rel}} - \sqrt{u_0})} * \frac{1}{Clockspeed} (\text{Eq. } 24)$$

A Mathcad document was created to calculate the optimal capacitance and inductor construction that maximizes resolution while maintaining the necessary magnitude of the signal slope at the second zero.

Cryogenic Behavior:

Circuit exposure to colder temperatures affects the circuit in two major ways: first, it reduces the resistivity of the copper wire significantly, and thereby the resistance per unit length,

θ, and second, it causes a small change in the period given a certain amount of insertion. The resistivity of a wire as a function of temperature is:

$$\rho(T) = \rho_0[1 + K^{-1}(T - T_0)] \quad (Eq. 25)$$

where ρ_0 is the initial resistivity, K^{-1} is the temperature coefficient, T_0 is the initial temperature in Kelvin, and T is the current temperature in Kelvin. From Eq. 25 the resistivity of copper wire at 20 K is 2.28% of its resistivity at room temperature, 273 K. Testing showed that the resistance drop was close to 10% from room temperature to 77 K. The major reduction in resistance results in less damping, and a more defined waveform. Therefore, an encoder operable only at lower temperatures can be constructed with more turns and a higher gauge wire while maintaining the same resolution. Inductor 5 was constructed near the size specifications needed for use in the laser-fusion target positioning system. Such construction requires the use of a higher gauge, smaller diameter wire, which has much higher resistance. In addition, the encoder required a smaller radius coil. To attain around the same period change and resolution the encoder required a greater number of turns. At room temperature the inductor signal did not oscillate due to a higher resistance and thus excessive damping. When tested in liquid nitrogen near 77 K, the resistance decreased, and the signal oscillated, yielding a resolution near 0.1 µm.

Exposure to cryogenic temperatures also changes the period given a certain amount of rod insertion. One of the desirables for the encoder was temperature independence, or the need not to recalibrate the encoder for each new operating temperature. An encoder whose change in period results in a difference in measurement readings greater than the stated resolution would require recalibration or a reevaluation of its resolution. The resistance change in addition to the decrease in inductance displayed in Figure 6 causes about a 0.5 mm error between cold and warm readings.

Inductor Number	Warm (mH) Retracted	Cold (mH) Retracted	$\frac{\Delta L}{Lwarm}$	Warm (mH) Inserted	Cold (mH) Inserted	$\frac{\Delta L}{Lwarm}$
5	12.706	12.102	-0.0475	70.787	69.4	-0.0196
3 at 120Hz	5.5671	5.5620	0.0000	50.804	48.813	-0.0392
3 at 1 KHz	5.789	5.6465	-0.0246	32.9036	28.612	-0.1304
Figure 6. The inductances of different inductors with the rod inserted and retracted at room temperature and 77 K. Generally, there is a decrease in inductance between warm and cold temperatures.						

Therefore, the encoder cannot have high resolution at both room and cryogenic temperatures as currently configured. The encoder construction results in higher resolution at warmer temperatures and lower resolution at colder temperatures. An encoder that is temperature independent must include a method for manual or sensor temperature input and a two-variable function that correlates the period input and temperature input to a certain amount of rod insertion. If temperature independence is not a requirement, the encoder can be constructed and calibrated to provide good resolution at a certain temperature.

Overall Device Functionality:

For each encoder, the time the op amp signal is high is correlated to the position of the magnetic rod. Data points correlating the position of the iron rod with the corresponding period of oscillation are shown in Figure 7 for inductor 4 by stepping the iron rod through the beginning 20 mm portion of the coil using a Keyence laser displacement measuring system.
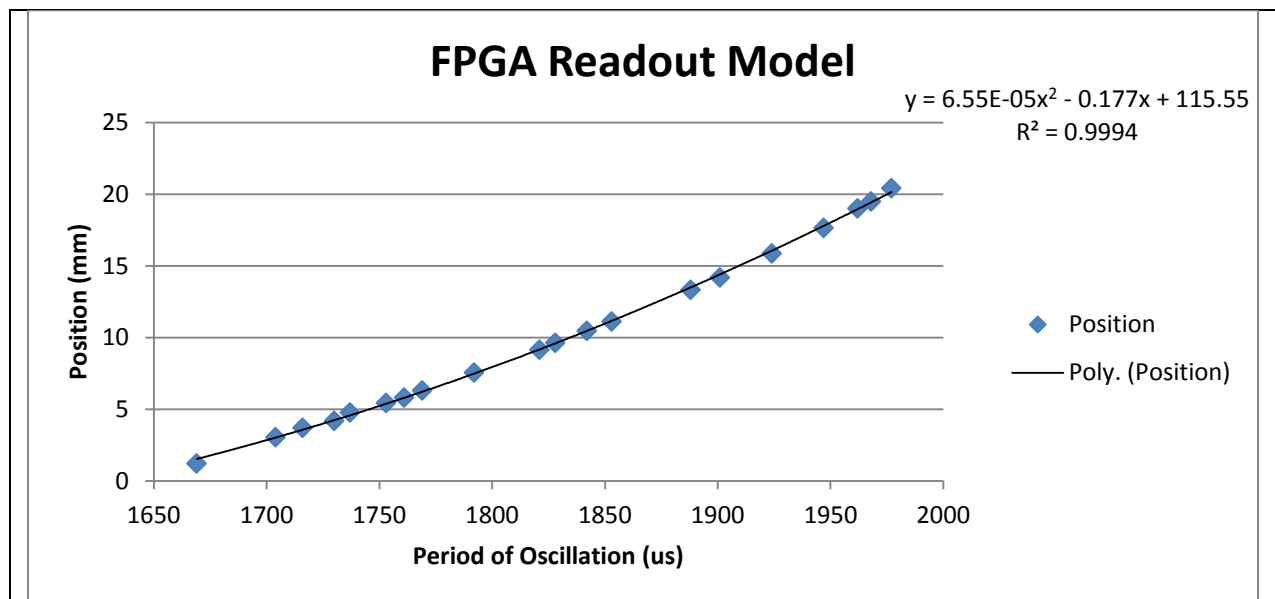
Figure 7. Correlation between the time the op amp signal is high and the position of the iron rod within the coil. For example, the FPGA would read a value such as 1873 μs, run it through the trend line formula and display a distance of 13.8 mm.

With the number of data points taken, the accuracy of the readout model for any position within the 20 mm inductor range tested was about 1 mm. More data points and a greater resolution would improve accuracy greatly. For a temperature-independent encoder, trend lines would have to be created for each new operating temperature. The trend lines could be modeled knowing the resistivity and inductance as a function of temperature. The resistivity as a function of temperature is provided in Eq. 25 above. The inductance as a function of temperature seems to depend on the permeability of the iron rod and the contraction of the coils to a smaller radius. Experiments have shown that the magnetic permeability of soft annealed Swedish iron decreases with decreasing temperature. For a magnetic force of 1.77 CGS tested, the permeability decreased linearly with decreasing temperature. The overall decrease from room temperature to 77 K was -17.7%. Though the annealed Swedish iron most accurately represents the manufacturing methods used for the M2 steel iron insert, it is also found that soft unannealed

Swedish iron had the opposite dependence on temperature, the permeability increasing with decreasing temperature. It was also found that the percentage change in permeability from cold to warm was dependent upon the amount of magnetic flux through the sample [3]. Similarly, Metglas shows temperature dependence decreasing from a u_{rel} value of 1,000,000 permeability at room temperature to 60,000 at 4.2 K. The contribution due to the copper coil contraction is orders of magnitudes smaller than the change seen in permeability. Thermal expansion data indicates that the percent change in length, which directly corresponds to the maximum possible percent change in radius, is -0.324%. The maximum coil contraction percentage contribution to the inductance percentage change is -0.649%. [4]

Conclusion:

An encoder concept was developed that combined a variable inductor, a ringing RLC circuit, an operational amplifier, and an FPGA. The insertion or retraction of a magnetically permeable rod into and out of a coil caused a change in inductance. This resulted in a change in the period of an oscillating RLC signal. The signal was converted into a square wave by way of an operational amplifier and a voltage offset system. An FPGA counted the time the signal was high, and correlated the count to a distance.

A relationship between inductor characteristics and circuit parameters was developed. The behavior of the RLC signal and the operational amplifier was characterized. It was found that the inductor's slope at the second zero and the op amp's fall time correlated. A Mathcad document was created to accurately calculate the optimal resolution, capacitance, and number of turns of the inductor given certain physical input parameters such as temperature, cross sectional area, length, and gauge.

With further improvement steps, the encoder has the potential to be a viable alternative to the currently used potentiometer solution. With the reduction of noise and more data points, the accuracy of a readout model could reach the measured resolution of 0.1 μm of the fifth inductor. Such accuracy would serve as an improvement over the current solution. With a more careful inductor construction, and sufficient calibration at the given operating temperature, an encoder can be constructed to replace the potentiometer solution.

References

[1]: Fawwaz T. Ulaby and Michel M. Maharbiz. Circuits. Allendale, NJ: National Technology & Science, 2009. Print.

[2]: Richard Palmer Reed and A. F. Clark. *Materials at Low Temperatures*. University of Michigan: American Society for Metals, 1983. Print.

[3]: J. Flemming and J. Dewar. "On the Magnetic Permeability and Hysteresis of Iron at Low Temperatures." Proceedings of the Royal Society of London 60 (1896): 81-95. Web. <http://archive.org/details/philtrans02805971>.

[4]: Hung P. Quach and Talso Chui. "Low Temperature Magnetic Properties of Metglas 2714A and Its Potential Use as Core Material for EM1 Filters." Jet Propulsion Laboratory, Califomia Institute of Technology Print.